ce/papers Proceedings in civil engineering

Ernst & Sohn A Wiley Brand

ORIGINAL ARTICLE

eurosteel AMSTERDAM 2023

Ernst & Sohn A Wiley Brand

An Analytical Design Approach for Outstand Steel Plates in Compression

Jurgen Becque[1]

Correspondence

Dr. Jurgen Becque
University of Cambridge
Department of Engineering
7a JJ Thomson Ave
Cambridge, CB3 0FA
Email: jurgen.becque@eng.cam.ac.uk

[1] University of Cambridge, Cambridge, UK

Abstract

Current design approaches to determine the capacity of plates in local buckling are based on empirical equations, in particular the widely used Winter equation. In contrast, this research presents a novel analytical approach, focusing on outstand steel plates. The derivation of the method is rooted in the Föppl-von Karman equations, which are first simplified by making a number of basic mechanical assumptions about the post-buckling stress field. An approximate solution to the emerging differential equation is obtained, which assumes a polynomial displacement profile in the transverse direction of the plate. This solution agrees eminently well with the results of finite element simulations, both for the case of a geometrically perfect plate and a plate containing an initial imperfection. By combining the obtained post-buckling stress profile with a failure criterion based on von Karman's effective width concept, a closed-form strength equation for compressed outstand plates is derived, which is seen to be a sole function of the plate slenderness and a dimensionless imperfection factor. This equation agrees closely with the available experimental data.

Keywords

Local buckling, Outstand plates, Post-buckling capacity, Unstiffened plates, Design

1 Introduction

The post-buckling behaviour of compressed plates is described by the Föppl-von Karman equations [1, 2], which comprise two coupled nonlinear partial differential equations:

$$D\left[\frac{\partial^4 w}{\partial x^4}+2\frac{\partial^4 w}{\partial x^2 y^2}+\frac{\partial^4 w}{\partial y^4}\right]=p_z$$
$$+t\left[\frac{\partial^2\phi}{\partial y^2}\frac{\partial^2(w+w_0)}{\partial x^2}-2\frac{\partial^2\phi}{\partial x\partial y}\frac{\partial^2(w+w_0)}{\partial x\partial y}+\frac{\partial^2\phi}{\partial x^2}\frac{\partial^2(w+w_0)}{\partial y^2}\right]$$

$$\left[\frac{\partial^4\phi}{\partial x^4}+2\frac{\partial^4\phi}{\partial x^2 y^2}+\frac{\partial^4\phi}{\partial y^4}\right]=$$

$$E\left[\left(\frac{\partial^2 w}{\partial x\partial y}\right)^2-\frac{\partial^2 w}{\partial x^2}\frac{\partial^2 w}{\partial y^2}+2\frac{\partial^2 w_0}{\partial x\partial y}\frac{\partial^2 w}{\partial x\partial y}-\frac{\partial^2 w_0}{\partial x^2}\frac{\partial^2 w}{\partial y^2}-\frac{\partial^2 w}{\partial x^2}\frac{\partial^2 w_0}{\partial y^2}\right] \quad (1)$$

In the above equations, ϕ is the Airy stress function, E is the elastic modulus, and p_z is the additional lateral (out-of-plane) pressure on the plate. It should be noted that the terms in w_0, which is the initial geometric imperfection, were actually added to the original Föppl-von Karman equations by Marguerre [3]. The constant D is the bending stiffness of the plate, given by:

$$D=\frac{Et^3}{12(1-\nu^2)} \quad (2)$$

In Eq. (2), t is the thickness of the plate and ν is the Poisson ratio of the material.

We will focus our attention on a rectangular plate with three simply supported sides and one free longitudinal edge, compressed uniformly at the ends, and with $p_z = 0$. For such a plate, no solution has yet been discovered to the Eqs. (1), despite more than a century having elapsed since their inception. Consequently, the practical design of such plates is instead governed by empirical equations. In particular, Eurocode EC3-1-5 [4] prescribes a modified Winter equation to calculate the capacity of a compressed outstand steel plate:

$$\frac{P_u}{P_y}=\frac{1}{\lambda}\left(1-\frac{0.188}{\lambda}\right) \quad (3)$$

In the above Eq. (3) P_u is the compressive capacity of the plate, P_y is its yield load, and the plate slenderness λ is given by its usual definition:

https://doi.org/10.1002/cepa.2535 wileyonlinelibrary.com/journal/cepa

$$\lambda = \sqrt{\frac{P_y}{P_{cr}}} \tag{4}$$

where P_{cr} is the (elastic) local buckling load.

This paper aims to connect theory and practice by deriving a Winter-type design equation, taking the Föppl-von Karman equations (Eqs. 1) as a starting point.

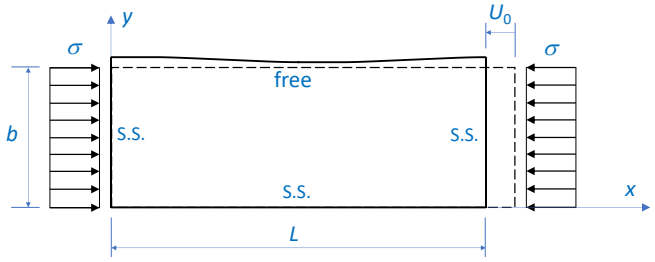

Figure 1 Boundary conditions and conventions (S.S. = simply supported)

2 Simplified differential equation

In order to achieve the aforementioned aim, Eqs. (1) are first simplified using the following two assumptions:

1. The longitudinal membrane stress σ_x does not depend on the longitudinal x-coordinate (see Fig. 1 for conventions). This means that the stress profile is identical in each transverse cross-section of the plate. This statement can be proven to be equivalent to Vlasov's assumption of zero membrane shear stress, extended into the post-buckling range.
2. The transverse membrane stresses σ_y are zero. This is believed to be a reasonable assumption, given that both the free and the simply supported longitudinal edge are unloaded in the transverse direction.

Using both assumptions, it can be proven that Eqs. (1) can be transformed into a single differential equation which no longer features the Airy stress function [5]. With the plate deflections w written as a multiplicative function:

$$w = Y(y).sin\left(\frac{\pi x}{L}\right) \tag{5}$$

this new differential equation becomes:

$$Y'''' - AY'' + BY + 2CYY_0^2 = -CY^3 - 3CY^2Y_0 + FY_0 \tag{6}$$

In Eq. (6), the constants A, B, C and F are defined as follows:

$$A = 2\left(\frac{\pi}{L}\right)^2$$

$$B = \left(\frac{\pi}{L}\right)^2\left[\left(\frac{\pi}{L}\right)^2 - \frac{2U_0}{\gamma}\right]$$

$$C = \frac{L}{2\gamma}\left(\frac{\pi}{L}\right)^4$$

$$F = \frac{2U_0}{\gamma}\left(\frac{\pi}{L}\right)^2 \tag{7}$$

In Eq. (7), U_0 is the uniform end shortening of the plate, L is its length, and the parameter γ is given by:

$$\gamma = \frac{2LD}{Et} = \frac{Lt^2}{6(1-\nu^2)} \tag{8}$$

Further to Eq. (6), $Y_0(y)$ indicates the shape of the initial imperfection in the transverse direction. In the longitudinal direction of the plate, the imperfection is assumed to have the shape of a half-sinewave.

Like the original Eqs. (1), from which Eq. (6) has been derived, elastic behaviour is implied in Eq. (6).

3 Solution technique

For the sake of simplicity, we assume that the initial imperfection has a straight transverse profile:

$$Y_0 = a_0 y \tag{9}$$

We then construct an approximate solution to Eq. (6) by proposing a deflected shape of the form:

$$Y = a_7y^7 + a_5y^5 + a_3y^3 + a_1y \tag{10}$$

where a_1, a_3, a_5 and a_7 are constant coefficients. It is seen that Eq. (10) automatically satisfies the boundary conditions along the longitudinally supported edge, namely:

$$w(y=0) = 0 \quad \Rightarrow \quad Y(0) = 0 \tag{11}$$

and:

$$M_y(y=0) = -D\left[\frac{\partial^2 w}{\partial y^2} + \nu\frac{\partial^2 w}{\partial x^2}\right]_{y=0} = -D\,w''(y=0) = 0 \tag{12}$$

Eq. (10) only contains odd powers of y, which is inspired by the observation that the problem in Fig. 1 can be extended by mirroring about the longitudinally supported edge, in which case the displacement pattern becomes anti-symmetric about this edge, while the stresses and displacements in the original plate remain unaltered.

One might also argue that proposing a 7-th order polynomial as a solution seems unnecessary, given that the transverse displacement profile for sufficiently long outstand plates is 'almost straight' [6]. However, two relationships between the a-coefficients are determined by the remaining boundary conditions, which leaves just two more degrees of freedom to obtain an optimal fit with Eq. (10). The remaining boundary conditions express zero moment and zero shear along the longitudinal edge and, based on classical plate theory, can be written as:

$$M_y(y=b) = 0 \quad \Rightarrow \quad \left[\frac{\partial^2 w}{\partial y^2} + \nu\frac{\partial^2 w}{\partial x^2}\right]_{y=b} = 0 \tag{13}$$

$$V_y(y=b) = 0 \quad \Rightarrow \quad \left[\frac{\partial^3 w}{\partial y^3} + (2-\nu)\frac{\partial^3 w}{\partial x^2 \partial y}\right]_{y=b} = 0 \tag{14}$$

Substituting Eq. (10) into Eqs. (13-14) results in:

$$a_7\left[42b^4-\nu\left(\frac{\pi}{L}\right)^2 b^6\right]+a_5\left[20b^2-\nu\left(\frac{\pi}{L}\right)^2 b^4\right]$$
$$+a_3\left[6-\nu\left(\frac{\pi}{L}\right)^2 b^2\right]-a_1\left[\nu\left(\frac{\pi}{L}\right)^2\right]=0 \quad (15)$$

and:

$$a_7\left[210b^4-7(2-\nu)\left(\frac{\pi}{L}\right)^2 b^6\right]+a_5\left[60b^2-5(2-\nu)\left(\frac{\pi}{L}\right)^2 b^4\right]$$
$$+a_3\left[6-3(2-\nu)\left(\frac{\pi}{L}\right)^2 b^2\right]-a_1\left[(2-\nu)\left(\frac{\pi}{L}\right)^2\right]=0 \quad (16)$$

On the other hand, we can also substitute the proposed solution (Eq. 10), together with Eq. (9), into the differential equation (Eq. 6). Retaining the lowest-order terms, in y and y^3, and requiring that their coefficients are zero leads to the following equations:

$$120a_5-6Aa_3+Ba_1=Fa_0 \quad (17)$$

$$840a_7-20Aa_5+Ba_3+2Ca_1a_0^2=-C(a_1)^3-3Ca_1^2a_0 \quad (18)$$

Neglecting the terms in y^5, as well as higher-order terms, is justified in this case, since the transverse displacement profile is known to be almost straight. Consequently, the term $a_1 y$ is the dominant term in Eq. (10). It can easily be verified that, upon substitution in Eq. (6), the coefficients of the higher-order terms contain products of the less important a-coefficients (i.e. those other than a_1) and are thus negligible.

Eqs. (15-18) form a system of four equations with four unknowns (a_1, a_3, a_5 and a_7), which is almost linear. Only Eq. (18) contains a cubic term in a_1. This implies that a_3, a_5 and a_7 can be expressed as a function of a_1 through manipulating Eqs. (15-17), and the results can then be substituted into Eq. (18) to yield a cubic equation in a_1. For a very long plate ($L \to \infty$) this equation becomes:

$$(a_1)^3+3a_0(a_1)^2+\frac{10\,L^2}{3b^2\pi^2}\left[\frac{1}{1+\nu}\left(\frac{t}{b}\right)^2-2\frac{U_0}{L}\right]a_1-\frac{20\,L}{3\pi^2b^2}U_0a_0=0 \quad (19)$$

Once the a-coefficients in Eq. (10) have been determined, the longitudinal stress profile follows from [5]:

$$\sigma_x=\frac{E}{2L}\left[\int_0^L\left[\left(\frac{\partial w}{\partial x}\right)^2+2\left(\frac{\partial w}{\partial x}\right)\left(\frac{\partial w_0}{\partial x}\right)\right]\mathrm{d}x-2U_0\right] \quad (20)$$

The compressive load P can subsequently be obtained by integrating these longitudinal stresses over the cross-section. Using Eqs. (20), (5) and (9), with Y=$a_1 y$, results in:

$$P=Ebt\frac{U_0}{L}-\frac{Et}{12}\left(\frac{\pi}{L}\right)^2 b^3(a_1^2+2a_1a_0) \quad (21)$$

It should be noted that for a theoretically infinitely long plate, all a-coefficients in Eq. (10) except a_1 tend to zero, so that the deflected plate is indeed straight in the transverse direction.

Eq. (19) provides a relationship between U_0 and a_1, so that Eq. (21) can then be called upon to expose either the load-shortening behaviour of the plate (P vs. U_0) or the load-deflection behaviour (P vs. $a_1 b$). These relationships were verified against a finite element (FE) model of an elastic outstand plate with b = 50 mm, L = 250 mm, t = 2 mm, E = 200 GPa and ν = 0.3. An imperfection was included in the shape of the first eigenmode (i.e. one displaying a single half-sine wave in the longitudinal direction) and an amplitude of 0.5 mm (= b/100 = L/500). The load-shortening behaviour and the load-deflection behaviour predicted by the FE model are shown in Figs. 2 and 3, respectively, and are compared to the theoretical predictions. To obtain the latter, Eq. (19) was solved for a range of U_0 values using Solver in Microsoft Excel [7]. The mid-length deflection was obtained as: $w_m = a_1 b$. It is seen from these figures that excellent agreement was obtained between the theory and the FE results over an extended range of post-buckling deformations. It is noted that the plate in the FE model has an aspect ratio of 5, while the theoretical solution pertains to an infinitely long plate.

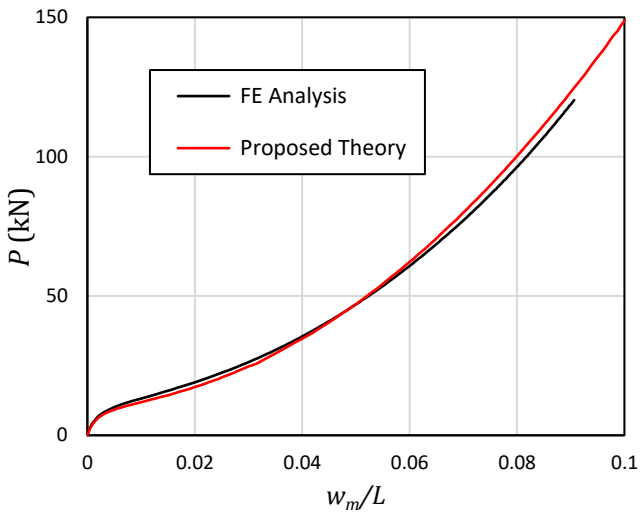

Figure 2 Load versus mid-length deflection along the free edge

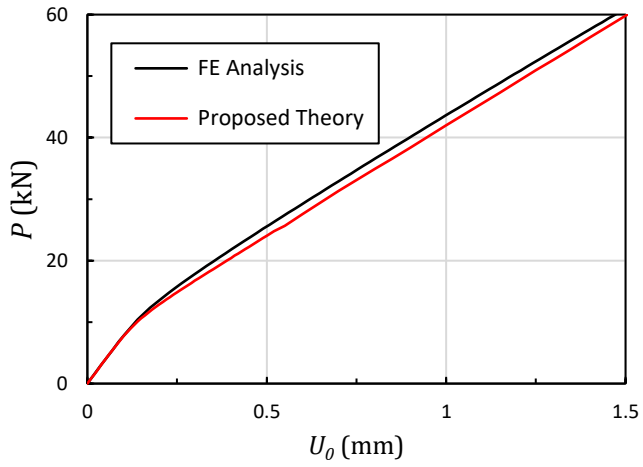

Figure 3 Load-shortening behaviour of an elastic outstand plate

4 Strength predictions

A prediction of the compressive capacity of outstand steel plates can be obtained by combining the above theory with a failure criterion. In particular, we assume that failure occurs when the maximum longitudinal membrane stress (occurring at $y = 0$) reaches the yield stress:

$$|\sigma_x|_{max} = \frac{EU_0}{L} = f_y \tag{22}$$

It is noted that Eq. (22) is essentially a reformulated version of von Karman's effective width concept.

Eq. (22) can be used to eliminate U_0 from Eqs. (19) and (21). The coefficient a_1 can subsequently also be algebraically eliminated from these two equations, leaving the following closed-form Winter-type strength equation:

$$\frac{1}{\lambda^2} = \left(\frac{9}{5}\frac{P_u}{P_y} - \frac{4}{5}\right)\left[1 + \frac{1}{\sqrt{1 + \frac{12}{\pi^2\alpha^2}\left(1 - \frac{P_u}{P_y}\right)} - 1}\right] + \frac{3\pi^2}{10}\alpha^2 \tag{23}$$

where the dimensionless imperfection factor α is given by:

$$\alpha = \sqrt{\frac{E}{f_y}}\frac{a_0 b}{L} \tag{24}$$

Eq. (23) has the potential to be used as a design equation, provided that a suitable value can be determined for the imperfection factor α. A quick sensitivity study reveals that Eq. (23) is quite insensitive to the value of the yield stress f_y in Eq. (24) within its typical range of values (i.e. f_y = 235-960 MPa). A typical value f_y = 350 MPa was therefore chosen. However, Eq. (23) is substantially more influenced by the choice of the geometric imperfection amplitude a_0. The European standard EN1090-2 [8], which relates to the practical execution of steel structures, specifies manufacturing tolerances for outstand plates comprising the flanges of welded steel I-beams. It stipulates that the maximum undulation over a gauge length L must be less than L /150. This provides a strong motivation to choose $a_0 b = L$ /150. The validity of this design approach was verified against experimental data available in literature, in particular: (i) 36 test results obtained at the University of Cambridge by Moxham [9], Rogers [10, 11] and Bradfield [12], (ii) 5 tests carried out by Nishino et al. [13], (iii) 6 tests by Rasmussen and Hancock [14], and (iv) 2 tests by Nie et al. [15]. Furthermore, 36 numerical results generated by Dinis and Camotim [16] were also considered. The latter were obtained using finite element simulations of cruciform columns with fixed end conditions, yield stresses ranging from 235 MPa to 1800 MPa, and initial imperfections in the shape of the critical buckling mode with an amplitude of 10% of the thickness. In order to also investigate the applicability of the proposed equation to aluminium, the results of 29 experiments on AA6082 cruciform columns, generated by Hopperstad [17] were added to the database.

Eq. (23) is compared to these 114 data points in Fig. 4, which also plots the EC3-1-5 design equation (Eq. 3). It is seen that the proposed analytical equation (Eq. 23) agrees very well with the experimental and numerical data. It mostly forms a lower bound to them, which is consistent with the rather conservative choice of the model imperfection as the manufacturing tolerance prescribed by the execution standard. Eq. (23) also agrees very well with the Eurocode design equation up to a slenderness λ = 1.5. Beyond this slenderness value, both curves start to diverge, with the newly proposed equation clearly providing the better agreement with the data. This illustrates the power of an analytical approach based on solid fundamentals, as opposed to empirical equations. It is noted that Winter did not have any data available in the higher slenderness range to calibrate his equation against.

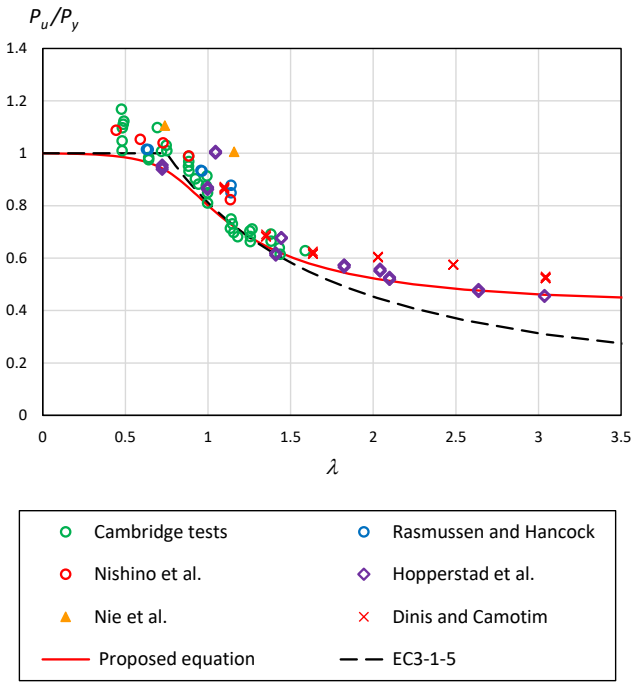

Figure 4 Comparison of proposed equation with experimental data

5 Conclusions

The development of an analytical method describing the post-buckling behaviour of rectangular outstand plates under longitudinal compression is presented in this paper. The Föppl-von Karman equations were taken as a starting point and were first simplified by adopting some basic assumptions about the stress field. The resulting differential equation was solved using a polynomial approximation for the transverse displacement profile, and the solution was shown to accurately represent the elastic post-buckling behaviour of outstand plates by means of a comparison with finite element analysis results.

A closed-form expression for the compressive capacity of an outstand steel plate was derived by introducing a failure criterion based on von Karman's effective width concept. This expression shows the dimensionless plate capacity P_u/P_y to be a sole function of the slenderness λ and a dimensionless imperfection factor α, in perfect analogy

with the Perry-Robertson column design curves. For an imperfection amplitude of $L/150$ and a yield stress of 350 MPa, this equation agrees exceedingly well with experimental and numerical data pertaining to steel and aluminium cruciform columns, up to a slenderness value of at least 3.0.

References

[1] Föppl, A. (1907) *Vorlesungen Über Technische Mechanik*. Druck und Verlag von B.G. Teubner.

[2] Von Karman, T. (1910) *Festigkeitsprobleme im Maschinenbau*. In: Klein, F., Müller, C., *Encyklopädie der Mathematischen Wissenschaften*. Druck und Verlag von B.G. Teubner, 311-385.

[3] Marguerre, K. (1939) *Zur Theorie der Gekrümten Platte Grosser Formänderung*. Proc., Fifth International Congress on Applied Mechanics, Cambridge, Massachusetts, J. Wiley and Sons, 93-101.

[4] CEN (2006) EN 1993-1-5: Eurocode 3: *Design of Steel Structures*, Part 1-5: *Plated Structural Elements*. European Committee for Standardization, Brussels.

[5] Becque, J. (2021) *Linking the von Karman equations to the practical design of plates*. ASCE Journal of Engineering Mechanics, 147(11), 04021097.

[6] Becque, J. (2016) *The application of plastic flow theory to inelastic column buckling*. International Journal of Mechanical Sciences, 111-112, 116-124.

[7] Microsoft (2021) Microsoft Excel, Office 365, Version 2022, Redmond, WA, USA.

[8] CEN (2008) EN 1090-2: *Execution of steel structures and aluminium structures*. Part 2: *Technical requirements for steel structures.* European Committee for Standardization, Brussels.

[9] Moxham, K.E. (1971) *Buckling tests on individual welded steel plates in compression*. Technical Report No. CUED/C-Struct/TR3, Cambridge University, Cambridge, UK.

[10] Rogers, N.A. (1975) *Compression tests on plain flat outstands*. Technical Report No. CUED/C-Struct/TR52, Cambridge University, Cambridge, UK.

[11] Rogers, N.A. (1975) *Outstand failure in stiffened steel compression panels*. Technical Report No. CUED/C-Struct/TR54, Cambridge University, Cambridge, UK.

[12] Bradfield, C.D. (1978) *The strength of rectangular outstands loaded in compression*. Technical Report No. CUED/C-Struct./TR75, Cambridge University, Cambridge, UK, 1978.

[13] Nishino, F.; Tall, L.; Okumura, T. (1968) *Residual stress and torsional buckling strength of H and cruciform columns.* Japanese Soc. Civil Engs., Transactions, No. 160, 75-87.

[14] Rasmussen, K.J.R.; Hancock, G.C. (1992) *Plate slenderness limits for high strength steel sections*. Journal of Constructional Steel Research, 23, 73-96.

[15] Nie, J.; Sugimoto, H.; Ono, K.; Miyashita, T.; Matsumura, M.; Okada, S. (2019) *An experimental study on the local buckling strength of an SBHS700 stub column with cruciform section.* Steel Construction, 12(2).

[16] Dinis, P.B.; Camotim, D. (2011) *Buckling, post-buckling and strength of cruciform columns*. Proceedings of the Annual Stability Conference, SSRC, Pennsylvania, USA.

[17] Hopperstad, O.S.; Langseth, M.; Tryland, T. (1999) *Ultimate strength of aluminium alloy outstands in compression: experiments and simplified analysis*. Thin-walled Structures, 34, 279-294.